2024 International Conference on Simulation of Semiconductor Processes and Devices (SISPAD) | 979-8-3315-1635-2/24/$31.00 ©2024 IEEE | DOI: 10.1109/SISPAD62626.2024.10733150

Simulation of qubits confined in pseudo magnetic field generated by strained graphene nanoribbon

Yusuke Hayashi and Satofumi Souma†
Department of Electrical and Electronic Engineering, Kobe University, Kobe 657-8501, Japan
†email: ssouma@harbor.kobe-u.ac.jp

***Abstract*—We propose a qubit device utilizing pseudo magnetic field generated by strain in zigzag graphene nanoribbon, where the deformation of graphene generates a pseudo-magnetic field and thereby localize electronic states. Our simulations based on the NEGF method have shown that deformation-induced localized states couple only with the higher subband originating from bulk graphene when the deformation is small. On the other hand, a larger deformation enables the localized states to couple even with the lowest subband originating from the edge states, leading to significant spin-splittings in the conductance dips and suggesting potential applications in spintronic devices, including spin qubit devices.**

I. Introduction

Graphene is a promising material for future electronics for its high mobility. Graphene can be easily strained due to its one atom thickness. It is known that changes in the distance between atoms induce an effective vector potential [1], which results in a pseudo-magnetic field (PMF). This, in turn, leads to the formation of Landau levels–discrete energy levels observed in a magnetic field. Such PMF-induced Landau levels have also been experimentally observed in a PMF exceeding 300 T [2]. Electronic devices that utilize the PMF have been proposed such as FETs [3, 4] and a qubit device [5] so far.

It is also known that carbon-based materials are suitable for qubit devices due to its small spin-orbit interaction and hyperfine interaction. To manipulate electrons as qubits, it is necessary to confine them in a quantum dot (QD) to discretize their energy levels in a way that can be accessed from external electrodes. For such purpose, graphene nanoribbons may be advantageous since they have quasi-one-dimensional geometries and various conduction characteristics depending on their edges and width [6]. In particular, zigzag graphene nanoribbons (ZGNRs) are attractive since the presence of spin-polarized edge states in ZGNRs [7] is expected to facilitate spin-selective electron injection from electrodes

Another viewpoint in realizing the qubit device is that it is necessary to cause the Rabi oscillation of confined electrons for quantum gate operations. However, AC magnetic field to induce Rabi oscillation is a challenge due to heating problems and difficulties to irradiate the local area with magnetic field. Instead, it is expected that the Rabi oscillation is realized in the situation that the electrons go back and forth in a magnetic gradient [8], where the faster quantum gate operations are expected in a larger magnetic gradient.

With the above mentioned motivation, in this paper we present a numerical simulation study based on non-equilibrium Green's function (NEGF) of the spin-dependent electronic transport in ZGNRs, where the strain-induced PMF leads to the QD confined states.

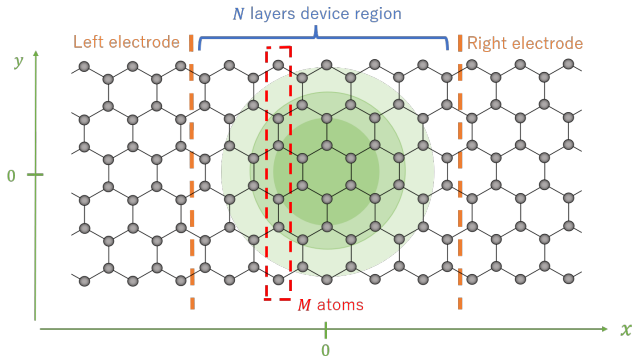

Fig. 1. The calculation model of ZGNR. We set x axis along the transport direction and the center of the device region is the origin. The semi-infinite ZGNR is attached to the both sides of the device region. The ripple strain (deformation) modeled by Eq. (1) is applied to the device region.

II. Model and Method

The calculation model of ZGNR is shown in Fig. 1. We set x axis along the transport direction and y axis the transverse direction. The origin is the center of the device region. We denote M the number of atoms along y axis in the device region and N along x axis, respectively. We choose $M = 12$ and $N = 61$, corresponding to the width $W = 2.41$ nm and the length $L = 7.38$ nm. The semi-infinite ZGNR electrodes are attached to the both sides of the device region. The ripple-type strain of the ZGNR can by modeled by the Gaussian deformation, where the displacement along the z direction for atoms located at (x, y) is given by

$$u_z(x, y) = h_0 e^{-\frac{x^2}{2\sigma_x^2} - \frac{y^2}{2\sigma_y^2}}, \tag{1}$$

with the parameters chosen to be $\sigma_x = 1.5$ nm, $\sigma_y = 1$ nm. The height parameter h_0 is treated as controllable parameter in this study. Then, in the framework of the tight-binding (TB) Hamiltonian the hopping energy between the nearest neighbor atoms is modeled as

$$t_{ij} = -t_0 e^{-\beta\left(\frac{d_{ij}}{a_0} - 1\right)}, \tag{2}$$

where $a_0 = 0.142$ nm and $t_0 = 2.8$ eV are the atomic distance and the hopping energy between the nearest neighbor

atoms in unstrained graphene, respectively, d_{ij} is the distance between nearest neighbor atoms labeled by i and j under the deformation Eq. (1), and $\beta \sim 3.37$ [9].

We note that the deformation Eq. (1) induces the corresponding in-plane displacements $u_{x,y}$ and thus the strain tensor ε_{ij}, which in turn results in the effective vector potential $\boldsymbol{A}$ as [1, 5]

$$\begin{pmatrix} A_x \\ A_y \end{pmatrix} = -\frac{\beta\hbar}{2ea_0}\begin{pmatrix} \varepsilon_{xx} - \varepsilon_{yy} \\ -2\varepsilon_{xy} \end{pmatrix}, \tag{3}$$

with ε_{ij} being the strain tensor. The corresponding PMF $\boldsymbol{B} = \nabla \times \boldsymbol{A}$ is shown in Fig. 2.

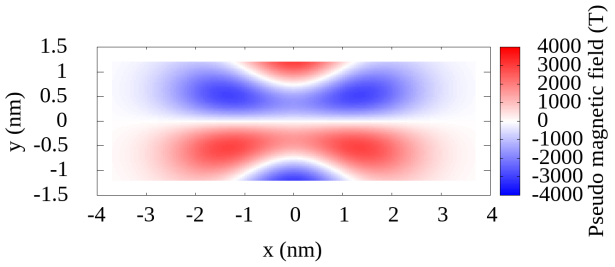

Fig. 2. The PMF that electrons in the K valley feel in strained ZGNR. The ripple parameter is chosen to be $h_0 = 0.5$ nm. The magnitude of the PMF can reach the thousands of Tesla.

For the actual NEGF transport calculation we employ the TB Hamiltonian for spin $\sigma(=\uparrow,\downarrow)$ in the device region as

$$H_{\mathrm{D}}^{\sigma} = H_{\mathrm{TB}} + V_{\mathrm{LSDA}}^{\sigma}. \tag{4}$$

The first term is the TB Hamiltonian with the hopping energy Eq. (1). The second term is the spin dependent exchange-correlation potential within the local spin density approximation [10–12].

We compute the density of states (DOS) and electron density self-consistently with the exchange-correlation potential in the NEGF formalism [12, 13]. The Green's function in the device region $G_{\mathrm{D}}(E)$ is defined as

$$G_{\mathrm{D}}^{\sigma}(E) = [E - H_{\mathrm{D}}^{\sigma} - \Sigma_{\mathrm{L}}^{\sigma}(E) - \Sigma_{\mathrm{R}}^{\sigma}(E)]^{-1}, \tag{5}$$

where $\Sigma_{\mathrm{L/R}}(E)$ is the self energy for spin σ from the left/right electrode and $E = 0$ is the Fermi energy. The retarded self energy $\Sigma_{\mathrm{L/R}}(E)$ is computed by the method proposed in Ref. [14]. At the ith site position $\boldsymbol{r} = \boldsymbol{r}_i$, the local density of states (LDOS) for spin σ, $D^{\sigma}(\boldsymbol{r}_i, E)$, is calculated by

$$D^{\sigma}(\boldsymbol{r}_i, E) = -\frac{\mathrm{Im}\,[G_{\mathrm{D}}^{\sigma}(E)]_{ii}}{\pi}, \tag{6}$$

where $[G_{\mathrm{D}}^{\sigma}(E)]_{ii}$ is the (i,i) matrix element of $G_{\mathrm{D}}^{\sigma}(E)$. The device DOS is defined as the averaged LDOS,

$$D(E) = \frac{1}{MN}\sum_{\sigma=\uparrow,\downarrow}\sum_{i} D^{\sigma}(\boldsymbol{r}_i, E). \tag{7}$$

The spin σ electron density at the position $\boldsymbol{r}_i$ is computed by

$$\rho_{\sigma}(\boldsymbol{r}_i) = \frac{1}{2\pi}\int dE\{[A_{\mathrm{L}}^{\sigma}(E)]_{ii}\, f(E-\mu_{\mathrm{L}}) + [A_{\mathrm{R}}^{\sigma}(E)]_{ii}\, f(E-\mu_{\mathrm{R}})\} \tag{8}$$

where $f(E)$ is the Fermi-Dirac distribution function with the electrochemical potential in the left/right electrode $\mu_{\mathrm{L/R}}$ set to zero assuming the zero bias limit and the temperature $T = 10$ K. $A_{\mathrm{L/R}}^{\sigma}(E)$ is the spectral function for electrons injected from the left/right electrode, given by

$$A_{\mathrm{L/R}}^{\sigma}(E) = G_{\mathrm{D}}^{\sigma}(E)\Gamma_{\mathrm{L/R}}^{\sigma}(E)\{G_{\mathrm{D}}^{\sigma}(E)\}^{\dagger}, \tag{9}$$

$$\Gamma_{\mathrm{L/R}}^{\sigma}(E) = i\left[\Sigma_{\mathrm{L/R}}^{\sigma}(E) - \{\Sigma_{\mathrm{L/R}}^{\sigma}(E)\}^{\dagger}\right]. \tag{10}$$

The spin dependent conductance is obtained by

$$G^{\sigma}(E) = \frac{e^2}{h}\mathrm{Tr}\left[\Gamma_{\mathrm{R}}^{\sigma}G_{\mathrm{D}}^{\sigma}(E)\Gamma_{\mathrm{L}}^{\sigma}\{G_{\mathrm{D}}^{\sigma}(E)\}^{\dagger}\right] \tag{11}$$

and the total conductance is calculated by

$$G(E) = \sum_{\sigma=\uparrow,\downarrow} G^{\sigma}(E). \tag{12}$$

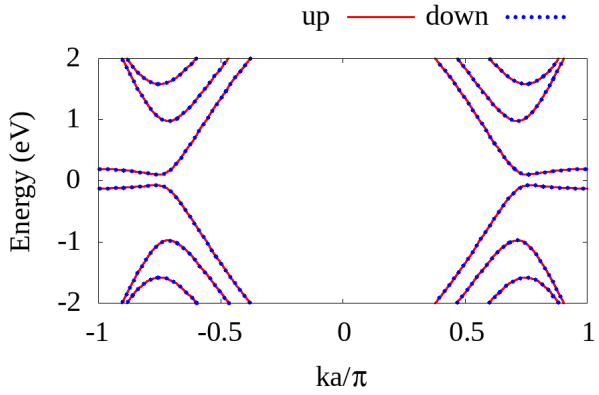

Fig. 3. The band structure of the electrode self-consistently solved for $h_0 = 0.5$ nm. The Fermi energy is $E = 0$. The bandgap is approximately 0.2 meV.

III. Results and Discussions

The band structure of the electrodes are shown in Fig. 3, where the finite bandgap approximately 0.2 eV is opened due to the exchange-correlation potential. We note that although the spin up and down band structures are identical, the corresponding wavefunctions differ from each other as will be shown later. Next we consider the DOS and in the device

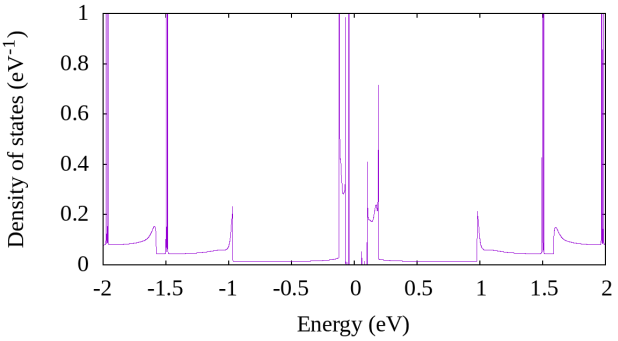

Fig. 4. The DOS for $h_0 = 0.5$ nm as a function of energy. Sharp peaks exist $E = \pm 1.5$ eV and $E = \pm 2.0$ eV in addition to the van-Hove singularity.

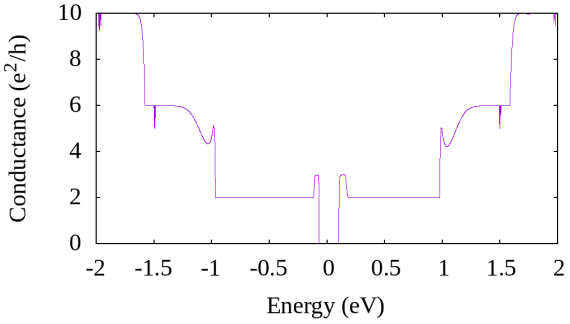

Fig. 5. The conductance for $h_0 = 0.5$ nm. The conductance dips are observed at the energy corresponding to the peaks of the DOS.

region with the strain (Gaussian deformation). Fig. 4 shows the DOS for the deformation height $h_0 = 0.5$ nm in the device region, where the peaks around $E \sim \pm 0.1$ eV are due to edge localized states, while those around $E \sim \pm 1$ is due to the van-Hove singularities seen in quasi 1D system in general. On the other hand, the additional peaks near $E \sim \pm 1.5$ eV and $E \sim \pm 2$ eV appear due to the Gaussian deformation, suggesting the presence of the deformation induced quasi localized states. Here we note that the localized state, for instance at $E = 1.5$ eV is degenerate with the second conduction subband (originating from bulk graphene band). As seen in Fig. 5, at the energy $E = 1.5$ eV the conductance exhibits a dip, which can be interpreted as the Fano resonance between the localized state at $E = 1.5$ eV and the extended band state. The same discussions can be applicable for other deformation induced DOS peaks.

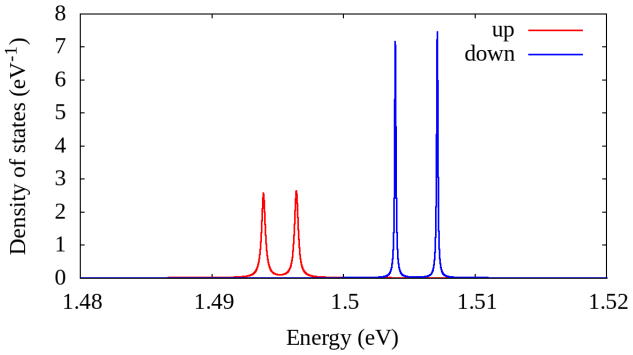

Fig. 6. The spin resolved DOS for $h_0 = 0.5$ nm as a function of energy. The energy splitting between the bonding and anti-bonding states of each spin is few meV. The splitting between the opposite spin is approximately 10 meV.

In order to understand the DOS peak/conductance dip structure at $E \sim 1.5$ eV more in detail, we show the spin resolved DOS for $h_0 = 0.5$ nm near $E = 1.5$ eV in Fig. 6. Here we can see the spin splitting ~ 10 meV, and for each spin the bonding/antibonding energy splitting with the coupling energy ~ 3 meV is observed. The corresponding spin dependent conductance $G^\sigma(E)$ and the conductance spin-polarization defined by $P = (G^\uparrow - G^\downarrow)/(G^\uparrow + G^\downarrow)$ are shown in Fig. 7 and Fig. 8, respectively. Here we can see that conductance is spin-polarized at the energy of the spin-splitted DOS peaks,

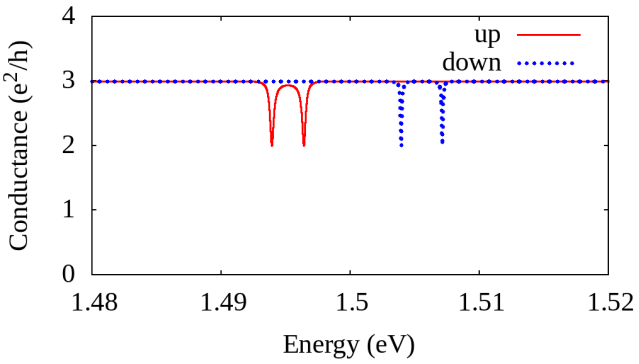

Fig. 7. The conductance of each spin for $h_0 = 0.5$ nm near the energy of the DOS peak around the $E = 1.5$ eV.

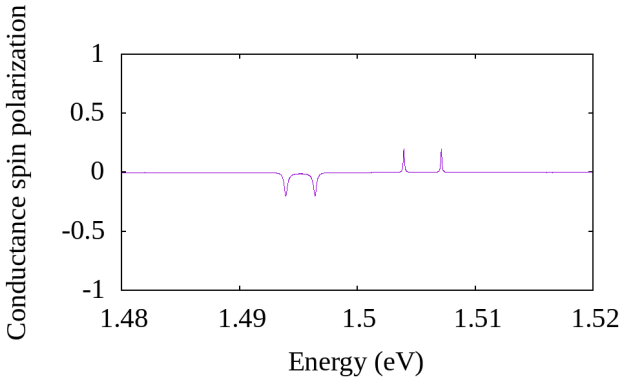

Fig. 8. The conductance spin polarization defined by $P = (G^\uparrow - G^\downarrow)/(G^\uparrow + G^\downarrow)$ for $h_0 = 0.5$ nm. The appearance of the peaks indicates the spin polarized current.

which can be utilized for applications in spintronic devices.

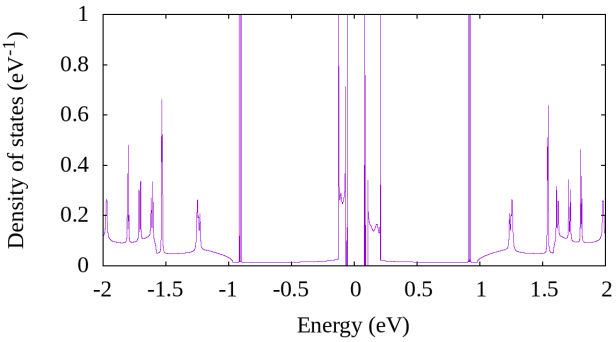

Fig. 9. The DOS for $h_0 = 0.85$ nm as a function of energy.

In the following, we consider the larger strain (deformation) case ($h_0 = 0.85$ nm). In Fig. 9, we show the total DOS for wider energy range $-2 \sim 2$ eV. In contrast to the small deformation height of $h_0 = 0.5$ nm (where the deformation-induced DOS peaks appear within the higher subband originating from the bulk graphene band), now in the case of $h_0 = 0.85$ nm, interestingly, additional DOS peaks are observed at $E \sim \pm 0.9$ eV which is within the lowest subband originating from the edge states (edge state subband). Here it is suggested that a larger deformation causes spatially more extended localized

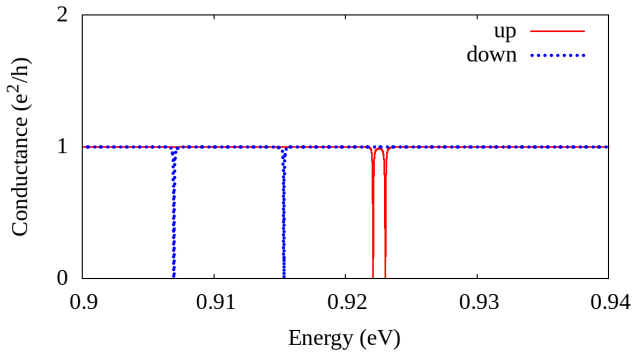

Fig. 10. The conductance near the DOS peaks at ~ 0.9 eV for $h_0 = 0.85$ nm. This energy range corresponds to the lowest subband (originating from the edge states). At the energy of the conductance dip, the perfect spin polarized transmission is realized.

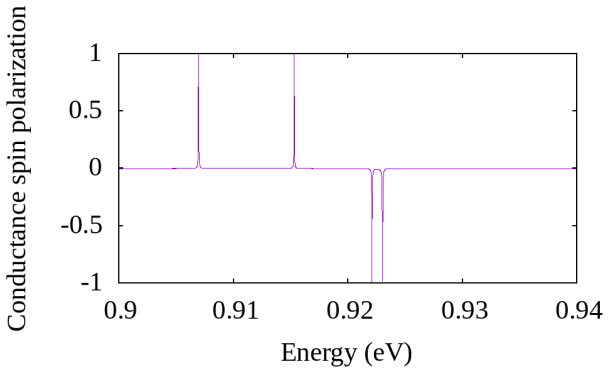

Fig. 11. The conductance spin polarization for $h_0 = 0.85$ nm.

states, making it possible for them to coupled even with the edge localized states. Therefore, as shown in Fig. 10, where we show the spin-resolved conductance near the DOS peaks at $E \sim 0.9$ eV, the conductance exhibit dips due to the Fano resonance mechanism. We note that there is only one conduction channel in this energy range, so at the energies of the spin-splitted conductance dips 100% conductance spin-polarization is obtained as shown in Fig. 11. We additionally comment that even for smaller deformation (e.g. $h_0 = 0.5$ nm), the DOS peaks associated with the edge-state subband can be observed if the center position of the Gaussian deformation is shifted along y axis (not shown in this paper).

We finally show the distribution of the spin polarization in Fig. 12, where the spin polarization $\zeta(\boldsymbol{r})$ is defined by

$$\zeta(\boldsymbol{r}) = \frac{\rho_\uparrow(\boldsymbol{r}) - \rho_\downarrow(\boldsymbol{r})}{\rho_\uparrow(\boldsymbol{r}) + \rho_\downarrow(\boldsymbol{r})}. \tag{13}$$

As shown in this figure, even if a large deformation $h_0 = 0.85$ nm is applied, one edge is polarized to up spin and the other to down spin, implying the validity of the interpretation described above. Moreover, it is implied that the co-existence of the edge-spin polarization and the edge-dependent PMF shown in Fig. 2 is the origin of the significant spin-dependent conductance shown in Fig. 10 and Fig. 11.

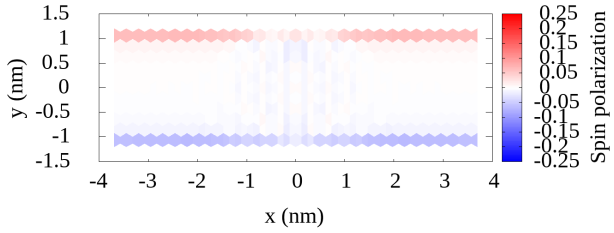

Fig. 12. The spatial distribution of spin polarization for $h_0 = 0.85$ nm. The upper edge is polarized to the up spin and the lower to the down spin.

IV. Conclusion

We have proposed a qubit device utilizing pseudo magnetic field generated by strain in zigzag graphene nanoribbon, where the deformation of graphene generates a pseudo-magnetic field and thereby localize electronic states. Our simulations based on the NEGF method have shown that deformation-induced localized states couple only with the higher subband originating from bulk graphene when the deformation is small. On the other hand, a larger deformation enables the localized states to couple even with the lowest subband originating from the edge states. This leads to significant spin-splittings (on the order of tens of meV) of the QD confined states, conductance dips, and perfect conductance spin-polarization, as well as bonding/anti-bonding splitting of a few meV. These findings suggest potential applications in spintronic devices, especially better noise resistant spin qubits.

References

[1] J. L. Mañes, Phys. Rev. B **76**, 045430 (2007).
[2] N. Levy, S. A. Burke, K. L. Meaker, M. Panlasigui, A. Zettl, F. Guinea, A. H. Castro Neto and M. F. Crommie, Science **329**, 5991 (2010).
[3] S. Souma, M. Ueyama and M. Ogawa, Appl. Phys. Lett. **104**, 213505 (2014).
[4] S. Souma and M. Ogawa, J. Appl. Phys. **127**, 094304 (2020).
[5] H. C. Park, J. Y. Han and N. Myoung, Quantum Sci. Technol. **8**, 025012 (2023).
[6] K. Wakabayashi, K. Sasaki, T. Nakanishi and T. Enoki, Sci. Technol. Adv. Mater. **11**, 054504 (2010).
[7] Y-W. Son, M. L. Cohen, S. G. Louie, Nature **444**, 347 (2006).
[8] Y. Tokura, W. G. van der Wiel, T. Obata and S. Tarucha, Phys. Rev. Lett. **96**, 047202 (2006).
[9] V. M. Pereira, A. H. Castro Neto and N. M. R. Peres, Phys. Rev. B **80** 045401 (2009).
[10] D. M. Ceperley and B. J. Alder, Phys. Rev. Lett. **45**, 566 (1980).
[11] J. Perdew and A. Zunger, Phys. Rev. B **23**, 5048 (1981).
[12] S. Souma, M. Ogawa, T. Yamamoto, and K. Watanabe, Proc. of 13th Int. Workshop on Comp. Electron. (IWCN-13), 81-84 (2009).
[13] C. H. Lewenkopf and E. R. Mucciolo, J. Comput. Electron. **12**, 203 (2013).
[14] T. Ando, Phys. Rev. B **44**, 8017 (1991).